RSC Advances

PAPER

View Article Online
View Journal | View Issue

Cite this: *RSC Adv.*, 2014, **4**, 31094

Spectral imaging of chemical reactions using a computer display and a digital camera†

Kai-Ta Hsieh[a] and Pawel L. Urban*[ab]

Various processes in chemistry lead to formation of spatial gradients, and cannot be directly studied using conventional spectroscopic techniques. Here we aimed to develop a simple method for the monitoring of light absorption at three wavelengths in two dimensions. The experimental setup consists of a commercial liquid crystal display (LCD) computer screen with light-emitting diode (LED) back illumination, and a digital camera equipped with a complementary metal oxide semiconductor imager. The computer screen serves as a multi-wavelength light source while the camera records distributions of the light transmitted through a two-dimensional non-homogeneous dynamic sample (reaction mixture). A program in C# language constantly changes the background colour of a console window, so as to alternately relay the light of different wavelength (λ_{max} = 608, 540, and 455 nm, respectively) onto the sample. The light emitted by the screen passes through a Petri dish containing the sample, while the digital camera records images revealing distributions of chemical substances absorbing at different wavelengths. The interval between two successive colour displays is 200–300 milliseconds. In this demonstration of the method, we followed two processes: the Belousov–Zhabotinsky oscillating reaction and the Old Nassau (Halloween) clock reaction. Every experiment produced a series of light absorption images corresponding to the wavelengths of the LCD/LED screen. Chemical front formation could be observed for analytes absorbing light at one of the three wavelength bands. In future, this approach can be extended to imaging at multiple wavelengths (by introducing customized LCD matrices and modified LED back illumination), and used in the monitoring of other non-homogeneous chemical processes.

Received 7th May 2014
Accepted 8th July 2014

DOI: 10.1039/c4ra04207g

www.rsc.org/advances

1. Introduction

Substance homogeneity is often assumed when studying artificial chemical systems. In synthesis, sufficient mixing of reagents warrants high efficiency, while inhomogeneities result in reduced production yields and give rise to system instabilities.[1] Likewise, non-homogeneous samples pose difficulties for analytical measurements. Analysis of such samples often leads to low precision and artefacts. Despite its undesirable characteristics, chemical heterogeneity rises curiosity of scientists. For example, the so-called "Hele-Shaw cell" enables observation of patterns in a quasi-two-dimensional environment which may involve reaction, diffusion, and convection.[2,3] In a recent study, temporal patterns of convection currents were characterised using segmented flow (preserving the information on the analyte distribution in a "convection chamber"), and the resulting discrete sample aliquots were analyzed on-line using a single-point flow-through optical detector.[4]

Apart from convection, many other chemical systems represent lack of spatial homogeneity and undergo temporal changes. In chemical reactions, concentrations of reactants evolve over time according to the kinetic characteristics of a given process.[5] Chemical oscillation is observed when a system does not follow simple progressive kinetics and reactants shuttle periodically between two or more quasi-stable states. Such chemical reaction systems are regarded as non-linear.[5,6] In 1958, a Russian chemist Boris Pavlovich Belousov discovered that the yellow colour of a mixture of bromate, citric acid and cerate vanished initially but reappeared after several minutes.[7] A revised version of the same reaction was published by Anatoly Markovich Zhabotinsky.[8] He replaced citric acid with malonic acid. Since then, variants of the proposed system have been referred to as the Belousov–Zhabotinsky (BZ) reaction. Interestingly, in an unstirred environment, the BZ mixture shows spatially extended phenomena of wave propagation, which can be explained with the reaction-diffusion mechanism.[9] This heterogeneous reaction system cannot be studied using standard methods (*e.g.* absorption spectroscopy) which are applicable to homogeneous samples.

Similar to chemical oscillations, clock reactions constitute a class of non-linear dynamic processes. They make prominent examples of non-equilibrium thermodynamics. The classical

[a]*Department of Applied Chemistry, National Chiao Tung University, Hsinchu 300, Taiwan*

[b]*Institute of Molecular Science, National Chiao Tung University, Hsinchu 300, Taiwan. E-mail: plurban@nctu.edu.tw*

† Electronic supplementary information (ESI) available: Additional Fig. (S1–S8); Movie S1 (blue, green, red). See DOI: 10.1039/c4ra04207g

iodine clock reaction was discovered by Hans Heinrich Landolt in 1886.[10] There are several variants of the iodine clock reaction. In the so-called "Old Nassau" (or "Halloween") reaction,[11] addition of mercury (Hg^{2+}) ions initially turns the reaction mixture yellow or orange (due to the formation of mercury iodide), and then blue (due to the formation of iodine–starch complexes).

The extensive use of ultraviolet-visible (UV-Vis) light absorption spectroscopy in various areas of chemical analysis can be attributed to its high throughput, precision, reliability, and quantitative capabilities.[12] In the standard format of UV-Vis absorption spectroscopy, a narrow light beam passes through the sample and its intensity is measured by a one-dimensional detector. Optical detectors based on this principle are widely used in conjunction with high-performance liquid chromatography (HPLC). Most such spectroscopic systems comprise a polychromatic source of light, a monochromator for wavelength selection, and a single- or multi-point sensor of light. State-of-the-art spectroscopic detectors for chromatographic separations incorporate light-emitting diodes (LEDs) as the sources of monochromatic light.[13] In general, spectroscopic UV-Vis detectors enable identification of sample components based on their characteristic absorption spectra as well as quantification of individual components. Most commercially available products do not have the capability to conduct simultaneous measurement in spectral, spatial, and temporal domain. Thus, this popular technique lacks the ability to characterize heterogeneous samples. In fact, the Lambert–Beer law – used as the basis of quantitative measurements in UV-Vis absorption spectroscopy – assumes perfect homogeneity of the sample.[12,14]

Taking into account the great interest in non-linear chemical systems discussed above, it is desirable to acquire the information on the distribution of analytes present in a heterogeneous sample. Therefore, there is a need for developing systems capable of mapping distributions of chemical substances in two and three-dimensional heterogeneous samples. One solution to this task could be the use of complementary metal oxide semiconductor (CMOS)-based digital camera as light detectors.[15,16] CMOS image sensors have comparable performance as popular charge-coupled devices (CCDs) in terms of noise, quantum efficiency, dynamic range, functionality, cost, and power consumption.[13]

Here we report construction of a facile system for mapping distributions of visible-light absorbing substances in two-dimensions, and recording these distributions in the time domain. The system can readily be assembled using widely available pieces of hardware and software: computer with LCD/LED screen, digital camera, and compiler of C#. We further demonstrate application of this system in the study of chemical processes: an oscillating reaction and a clock reaction.

2. Experimental section

2.1. Materials

1,4-Cyclohexanedione (CHD), mercury(II) chloride, potassium iodate, sodium bromate, sodium bromide, and sodium metabisulfite were purchased from Sigma-Aldrich (St Louis, MO, USA). Ferroin indicator solution (without chloride ions) was purchased from Fluka (St Louis, MO, USA).

2.2. Spatiotemporal three-wavelength imaging system

The imaging system incorporates a commercial CMOS-based digital camera (P7700, Nikon, Tokyo, Japan), a glass Petri dish – acting as sample chamber – and an LCD computer screen with LED back illumination (VM247T, ASUSTeK; Taipei, Taiwan) connected to a personal computer (Fig. 1). The LCD/LED screen plays the role of light source, while the CMOS camera is used as detector. In order to provide homogeneous illumination at three different wavelengths, a program was written in C# language (.NET Framework 4.5.1, Microsoft, Albuquerque, NM, USA). This program manages presentation of the background of the console window (see Fig. S1† for the flow chart), changing the colour alternately among red, blue, and green with the interval of 200–300 milliseconds (depending on experiment). The property *Console.BackgroundColor* was used for that purpose. In a preliminary test, visible light spectra were obtained for different colour channels of the LCD screen (Fig. S2†). This measurement was conducted using a miniature fibre optic spectrophotometer (Ocean Optics, Dunedin, FL, USA). During the reaction monitoring, a glass Petri dish (inner diameter: 89 mm; thickness of glass: 1.5 mm) – containing a thin layer of the reaction mixture – was laid directly on top of the horizontally arranged LCD screen. The progress of the reaction was recorded by the digital camera, which resulted in a video file. The experiment was carried out in a relatively dark environment in order to prevent any major influence of the ambient light.

2.3. Data processing

The video sequence obtained during the reaction monitoring (see Section 2.2) was split into individual frames. The obtained sets of data included images revealing light absorption patterns at three different wavelengths (*cf.* Fig. S2†). Data processing was conducted using programs written in C#, according to the algorithms illustrated in Fig. S3 and S4,† executed sequentially. In essence, all the images were separated into three groups

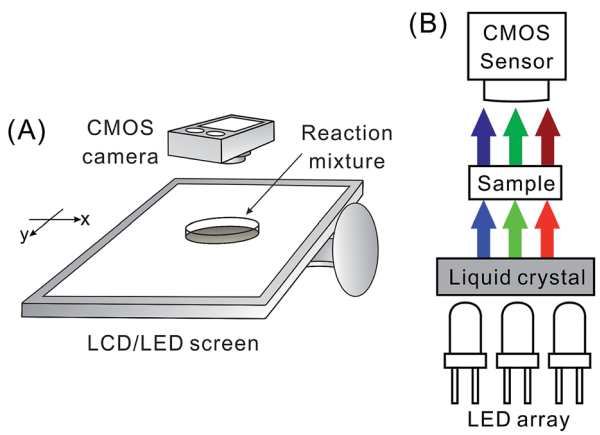

Fig. 1 Experimental system for spatiotemporal imaging at three wavelengths. (A) Layout; and (B) cross-sectional view.

according to their background colours. Changes of blue and red channel intensities of the RGB colour space were used to decide the start and the end of a group. A group was composed of several images which were attributed to a single time point. Due to the frame rate of the CMOS camera (30 frames per second), there were 8 to 10 frames (when the wavelength presentation time was set to 300 ms) for each of the three wavelengths at every time point. The frame corresponding to the middle of the sampling interval was chosen as the representative frame (typically, frame no. 4, 5, or 6, when the wavelength presentation time was set to 300 ms). For each representative frame, the extraction of RGB values (for every pixel along a line of interest) was conducted using the algorithm illustrated in Fig. S4.† First, the program calculates the slope and the intercept of a linear function describing a line joining two points which are arbitrarily selected by the user. Second, the program creates a matrix with co-ordinates of pixels which are located closest to the line described by the obtained linear equation. Third, based on this list of co-ordinates, the program extracts the RGB values of the corresponding pixels. This sequence is repeated for every representative frame. The exported RGB value matrix is transformed into absorbance matrix using the formula derived from the Beer's law,[12] similarly as it is done in a previously published UV imaging method[16]

$$A = \log_{10} \frac{(I_0/I)_s}{(I_0/I)_{ref}} \quad (1)$$

where I denotes the intensity of signal (sum of R, G, and B values) measured for a given wavelength (colour of the screen). The subscript 's' indicates that the value was obtained from

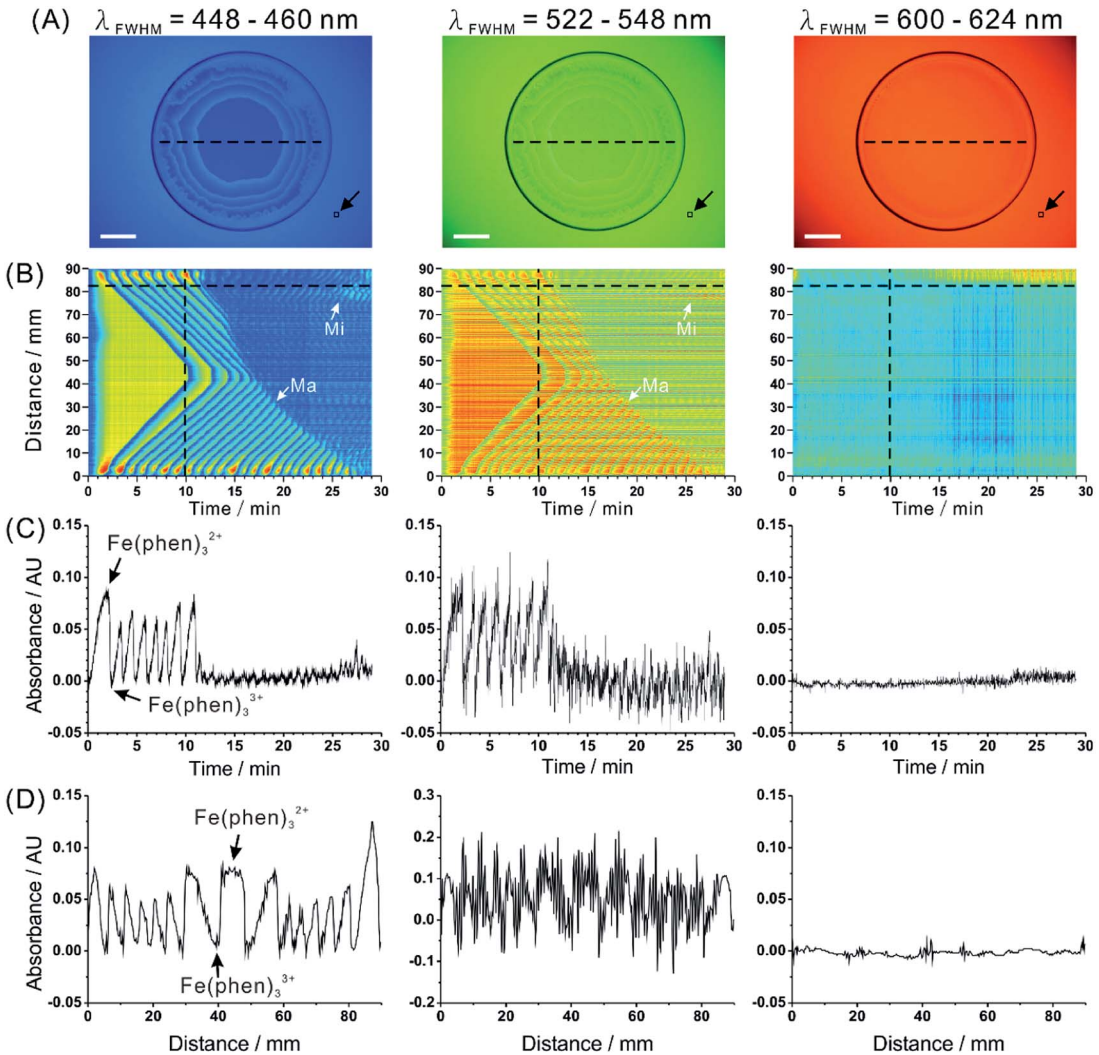

Fig. 2 Spatiotemporal characteristics of Belousov–Zhabotinsky reaction captured by the proposed imaging system. (A) Real images obtained at three wavelength bands. Glass Petri dish contains the BZ reaction mixture (6 mL). Scale bars: 2 cm. See Movie S1† (blue, green, red) to view the corresponding sequence (speed: 20×). (B) Spatiotemporal data for a selected intersect (*cf.* dashed line in (A)). White arrows indicate representative reaction fronts corresponding to major (Ma) oscillations and minor (Mi) oscillations. (C) Dependence of absorbance on time for a selected pixel (*cf.* horizontal dashed line in (B)). (D) Dependence of absorbance on distance for a selected time point (*cf.* vertical dashed line in (B)). Black arrow in (A) points to the reference zone (10 × 10 pixels). Arrows in (C) and (D) indicate the two colour forms of the reaction products which give rise to the observable waves. See Fig. S7† for the results of a blank measurement.

pixels in each representative frame and the subscript 'ref' indicates that the data was from the average of reference pixels, the position of which is indicated in Fig. 2 and 3. The subscript '0' indicates the signal intensity obtained from pixels in the first representative frame – corresponding to the reaction mixture before the light-absorbing waves develop.

Absorbance values calculated using eqn (1) were exported – by means of the algorithm illustrated in Fig. S4† – into an Excel (2013, Microsoft, WA, USA) spreadsheet. A two-dimensional data matrix was composed of absorbances of individual pixels (column) at every time point (row). Colour maps relating the absorbance values with the distance measured along a pre-selected intersect line and time, were plotted in the MATLAB software (2013b, MathWorks, MO, USA). Two-dimensional graphs at either distinct time points or distances were plotted in the Origin software (v8.0724, OriginLab, MA, USA) to demonstrate temporal and spatial profiling of the studied dynamic heterogeneous systems.

2.4. Oscillating reaction

A modified version of the Belousov–Zhabotinsky (BZ) reaction[17] featuring its bubble-free characteristic was performed. A mechanism of this variant was proposed by Basavaraja *et al.*[18] who summarized the underlying transformations in the following chemical equations:

$$Fe(phen)_3^{2+} + BrO_2^{\cdot} + H^+ \rightarrow Fe(phen)_3^{3+} + HBrO_2 \quad (2)$$

$$2Fe(phen)_3^{3+} + CHD \rightarrow H_2Q + 2H^+ + 2Fe(phen)_3^{2+} \quad (3)$$

1,10-Phenanthroline (phen) is a bidentate ligand which can chelate with ferrous or ferric ion, and form two species absorbing light at different wavelengths. Bromate ion and 1,4-cyclohexanedione (CHD) play essential roles in this redox process. Hydroquinone (H_2Q) contributes to the reaction in the

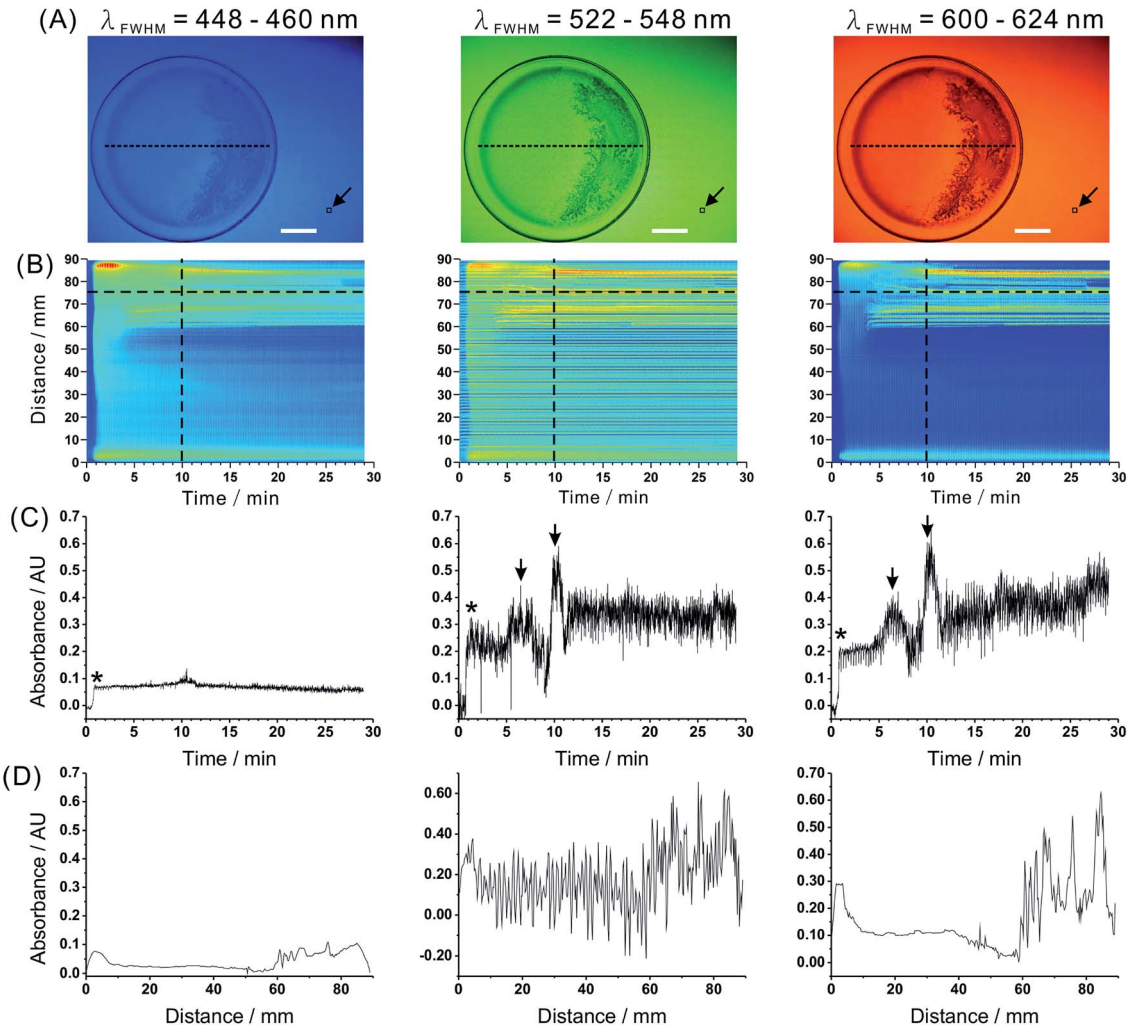

Fig. 3 Spatiotemporal characteristics of the Old Nassau reaction captured by the proposed imaging system. (A) Real images obtained at three wavelength bands. Glass Petri dish contains the Old Nassau reaction mixture (6 mL). Scale bars: 2 cm. (B) Spatiotemporal data for a selected intersect (*cf.* dashed line in (A)). (C) Dependence of absorbance on time for a selected pixel (*cf.* horizontal dashed line in (B)). (D) Dependence of absorbance on distance for a selected time point (*cf.* vertical dashed line in (B)). Black arrow in (A) points to the reference zone (10 × 10 pixels). Asterisks (*) in (C) indicate the formation of blue triiodide–starch complex. Arrows in (C) indicate iodine precipitate. See Fig. S8† for the results of a blank measurement.

auto-catalytic loop, and triggers the oscillation when its concentration reaches the critical value.[18]

Firstly, two substrate solutions were prepared as follows: solution A consists of sulphuric acid (0.60 mol L^{-1}) and sodium bromate (0.60 mol L^{-1}); solution B contains sodium bromide (0.11 mol L^{-1}) and 1,4-cyclohexanedione (0.40 mol L^{-1}). Subsequently, equal volumes of the solution A and the solution B were poured into a beaker, and the mixture was stirred. After ~5 s, the resulting mixture turned yellow due to the formation of Br_2. Finally, ferroin indicator solution (0.63 mol L^{-1}) was added to the mixture. After 2 h of stirring, the reaction mixture was transferred into a glass Petri dish with the thickness of the liquid being ~1.0 mm (calculated). The reaction started with the change of colour from light-blue to orange-red, and revealed propagating chemical waves, which resulted in the characteristic "fractal" patterns.

2.5. Clock reaction

The reagents used to perform the Old Nassau reaction are: potassium iodate, sodium metabisulfite, mercury(II) chloride, and starch. First, the following aqueous solutions were prepared: solution A ($[KIO_3]$ = 0.070 mol L^{-1}), solution B ($[Na_2S_2O_5]$ = 0.072 mol L^{-1} and [starch] = 4.0 g L^{-1}), and solution C ($[HgCl_2]$ = 0.011 mol L^{-1}). Next, equal amounts of the three solutions were poured into a beaker. The mixture was then transferred into the glass Petri dish. Shaking and stirring of the reaction mixture was avoided while handling it. The following equations summarize the mechanism of the Old Nassau reaction.[10]

$$IO_3^- + 3HSO_3^- \rightarrow I^- + 3SO_4^{2-} + 3H^+ \quad (4)$$

$$Hg^{2+} + 2I^- \rightarrow HgI_2 \quad (5)$$

$$IO_3^- + 5I^- + 6H^+ \rightarrow 3I_2 + 3H_2O \quad (6)$$

$$I_2 + HSO_3^- + H_2O \rightarrow 2I^- + SO_4^{2-} + 3H^+ \quad (7)$$

$$I_2 + I^- + \text{starch} \rightarrow \text{blue/black complex} \quad (8)$$

3. Results and discussion

3.1. Construction and characterisation of the experimental system

To enable spatiotemporal and spectral monitoring of the selected non-linear reactions, flashes of light at different wavelengths were emitted by the LCD/LED computer screen, and the transmitted light was recorded by the digital CMOS camera. The digital camera and the monitor screen were arranged in a way that the angle between their base edges was ~45°, which helped to prevent formation of excessive noise patterns.

In general, RGB colour space/model is widely used to reproduce the palette of colours in various types of image sensors and output devices.[19] However, as it is a device-dependent colour model, different output devices may generate a distinct colour given the same RGB values. In this study, the LCD/LED screen was used as a source of monochromatised light. The wavelength ranges of the three emission bands (see Fig. S2† for emission spectra) – calculated based on the full width at half maximum (FWHM) – are 448–460 nm, 522–548 nm, and 600–624 nm respectively. Although the FWHM of the three wavelength bands do not overlap, the emission bands (inspected at their bases) show a slight overlap. This might hinder the ability of the experimental system to distinguish analytes based on their spectral characteristics in the situations where the differences between the absorption maxima are small. The results described below reveal satisfactory wavelength selectivity of the liquid crystal display (LCD) for the chosen reaction systems. It should also be noted that the emission bands of the LCD/LED display may be narrower than the absorption bands of the filters in the common types of CMOS sensors employed in digital cameras (see, for example[20]). Therefore, using the LCD/LED display as the source of light in absorption measurement might provide better selectivity than only using a digital camera. Nonetheless, one shall not exclude the possibility that using high-quality colour imagers (with narrow-band filters), along with polychromatic illumination, might provide comparable or better results.

In order to verify the reproducibility of the proposed monitoring method, we measured absorbance values of a ferroin solution ([ferroin] = 0.63 mmol L^{-1}). The interval between two adjacent representative frames was set to 1 s, and the total duration of the measurement was 29 min. For each representative frame, the mean absorbance value and colour intensity (sum of the three RGB colour channels) were determined from 100 pixels within the zone of the Petri dish. The standard deviations of absorbance determined for the 3 channels were 2.54 (448–460 nm), 6.26 (522–548 nm), and 2.49 (600–624 nm) mAU. Average values of the RGB colour intensities (for the blank of the BZ reaction) were 304, 298 and 342; standard deviations were 3.5, 8.7, and 7.1 respectively. Dark images were recorded when the back light of the computer screen was off. Average and standard deviation of the colour intensity in these dark images were 7.5 and 1.5, respectively. This result shows the presence of minor instabilities of light intensity which may be attributed to rapid switching between the three different colours, and the influence of ambient light. Since the average intensity values of the dark images were small, they were not subtracted from the experimental data processed according to eqn (1).

Furthermore, a series of ferroin solutions (0.025–5.0 mmol L^{-1}) were measured by the proposed system. Fig. S5† shows the absorbance/concentration dependences at three wavelength bands. As expected, the increase of ferroin concentration decreases the intensity of light transmitted through the sample in the blue light channel. Note well, the ferroin absorption maximum is 512 nm (Fig. S6†) but the observed absorption band appears asymmetrical, extending more towards shorter wavelengths than to longer wavelengths. Therefore, a higher slope of the calibration curve is observed in the case of blue light (448–460 nm) than in the case of green light (522–548 nm). The decrease of the apparent absorbance in red light may be explained with a possible change of refractive index of the sample at higher concentration, and flattening of the liquid layer in the centre of the Petri dish due to the presence of

adhesive forces. Overall, the system provides a dynamic range of 2 magnitude (0.025–5.0 mmol L^{-1} ferroin). The estimated limit of detection (LOD) for ferroin is 0.175 mmol L^{-1}. A lower concentration LOD may be obtained following an increase of the optical path length (thicker layer of sample in the Petri dish). However, this would complicate the monitoring system by increasing contribution of the waves formed in the direction perpendicular to the imaged surface.

3.2. Application in the monitoring of an oscillating reaction

The progress of BZ reaction was captured in a 29 min long film, in which the three wavelength-specific images are separated following the data processing (Movie S1,† blue, green, red). The blue spherical rings expand in an initially homogeneous disk of the red-coloured solution. The colour change arises from the redox reaction between ferroin ($Fe(phen)_3^{2+}$, red) and its ferric derivative ($Fe(phen)_3^{3+}$, blue). As shown in the real images (Fig. 2A), oscillation patterns could readily be visualized at blue (448–460 nm) and green (522–548 nm) back light provided by the computer screen. Due to the fact that a coloured substance absorbs the light of complementary colour, the dark regions – in the blue and green images – correspond to the reduced form of ferroin ($Fe(o\text{-phen})_3^{2+}$), while the transparent regions correspond to the oxidized form of ferroin ($Fe(phen)_3^{3+}$). However, these oscillation patterns could not be observed at red (600–624 nm) back light because of the pale blue colour as well as insufficient optical path length.

We further illustrated spatiotemporal characteristics of BZ reaction by mapping the absorbance value of every point on the intersect line (*cf.* dashed black line in Fig. 2A) along the time axis (Fig. 2B). In the beginning, one could observe the absorbance changed in the bulk of the solution present in the reaction vessel. Afterwards, the waves developed and advanced towards the centre of the Petri dish. The 2D "survey map" clearly shows the propagation of chemical waves produced by BZ reaction. While the two transient reactants have no or little absorption in 600–624 nm wavelength range, it is easy to see them in the absorption maps for 448–460 nm and 522–548 nm wavelength ranges. We noticed prominent noise for the green (522–548 nm wavelength range) back light. This noise is probably related to a mismatch between the LCD filter array in the screen and the CMOS sensor array in the camera. Temporal profile of the reaction obtained for a selected pixel (located at ~82 mm from the initial point of the intersect line) is shown in Fig. 2C. In this graph, periodic oscillations between two major compounds are observed for 448–460 nm and 522–548 nm wavelength ranges. It is also noticeable that the amplitude of the oscillation waves changes over time. In the first 10 min, major oscillations (Fig. 2B, Ma) could be observed with changes of absorbance more than 0.05 AU (peak-to-peak). After 10 min, the amplitude of oscillation decreased to a great extent; however, some minor oscillations (Fig. 2B, Mi) could still be recorded. This phenomenon was hardly observable by naked eyes. Spatial profiles for three wavelength channels at a selected time point (the 10^{th} minute) are plotted in Fig. 2D. The waves present nearly symmetrical geometry, which corresponds to the circular (major) waves due to the propagation of the BZ reaction fronts advancing towards the centre of the container. Bigger peak-to-peak distances in the centre region indicate the direction of the propagation (from the edge towards the centre). A blank experiment was carried out to confirm that the oscillations discussed above (major and minor) are attributed to the BZ reaction (see Fig. S7†).

In this first demonstration, light-emitting diodes, liquid crystal display, and CMOS sensor were combined together to provide a wavelength selection for the monitoring of a multi-component non-homogeneous reaction system. LCD screen is an efficient and inexpensive way of generating pulses of relatively monochromatic light. Such illumination has relatively good homogeneity over centimetre-range distances; therefore, it can be used to monitor reaction vessels with large cross-section (*e.g.* Petri dish). The apparent inhomogeneity in Fig. 2A and B is due to the unequal distance of the CMOS imager from the points on the surface of the screen (centre *vs.* edge). However, this intensity profile does not significantly affect absorbance distribution since the intensity differences are cancelled when using eqn (1). Nonetheless, LCD/LED screen is not meant as a replacement for expensive multi-wavelength illumination systems for spectral imaging in fluorescence microscopy.[21]

There have been several examples of using CMOS- and CCD-based digital cameras in analytical chemistry, in the measurements of visible light. For example, da Nobrega Gaiao *et al.* introduced image-based titration enabled by digital camera.[22] In other work, Silva Lyra *et al.* used digital camera to acquire data in flame emission spectrometry.[23] A recent article reported on the use of digital camera as the detector of chemiluminescence.[24] In addition, Petryayeva *et al.* developed a FRET-based assay to determine proteolytic activity using CMOS cameras in smartphones.[25] By interpreting RGB intensities obtained from images, proteolytic activities of three different proteases could be assessed at the same time. The current study – along with the previous studies – show a great potential of digital imagers (for example, those based on CMOS) in visible-range spectrophotometric analyses.

3.3. Application in the monitoring of a clock reaction

To further demonstrate the usefulness of the proposed detection setup in the monitoring of non-homogeneous processes, we utilized it in the visualization of another non-linear process – the Old Nassau reaction. In order to increase temporal resolution of the monitoring, we decreased the wavelength-presentation interval from 300 to 200 ms. Real images of the reaction mixture at three different wavelength ranges are shown in Fig. 3A. The reference points were the same as in the previous experiment (Fig. 2A). In the images obtained for the Old Nassau reaction, one can observe formation of the solid precipitate (right-hand side of the Petri dish). Similarly to Fig. 2, absorbance values along the intersect line at every time point were mapped in Fig. 3B. The increase of absorbance at ~1 min corresponds to the formation of the blue tri-iodide–starch complex. Temporal profiles and spatial distributions were illustrated in Fig. 3C and D, respectively. Two prominent peaks

(highlighted with arrows) correspond to iodine precipitates. The absorbance values in the wavelength ranges 522–548 and 600–624 nm are much higher than those recorded in the wavelength range 448–460 nm because the blue tri-iodide–starch complexes do not strongly absorb/scatter blue light. The temporal and spatial properties of the Old Nassau reaction seems to be stochastic. It may be influenced by experimental conditions which cannot be fully controlled (for example, formation of temperature gradients in and at the reaction chamber).

In this work, we implemented spectral imaging to a less studied non-linear reaction system (the Old Nassau reaction). This application shows the usefulness of the proposed experimental approach in the monitoring of such processes, and we hope it can be applied to other systems in which spatiotemporal waves of chromogenic reactants develop, and/or reaction by-products precipitate.

4. Conclusions

In this proof-of-concept study, dynamic imaging and monitoring of chemical reactions was carried out using an LCD/LED computer display and a CMOS digital camera. In a series of tests, satisfactory reliability and reproducibility of this method has been confirmed. Subsequently, using this method, we were able to obtain spatial, temporal, and spectral information on the progress of oscillating and clock reactions. In the case of the BZ reaction, both major and minor waves could be observed. The method provides temporal resolution in the order of $\leq$1 s, which is suitable for real-time analysis of many non-linear chemical systems. The spatial resolution of the imaging system is estimated to be $\leq$0.25 mm, which is satisfactory for imaging macroscopic reaction vessels (Petri dish). On the other hand, since only a small number of compounds absorb visible light, the application of this method is limited to the wavelengths within the range 400–700 nm. In future, this disadvantage may be eliminated by constructing screens equipped with LCD matrices with several (>3) filters and introducing LEDs with different emission wavelengths. In the present work, we applied homogenous illumination to reaction vessels. However, structuring light-emitting zones within the LCD/LED display may provide additional benefits while monitoring microfluidic microreactors. An increased spectral coverage could then be achieved while preserving spatial arrangement of microscale reaction compartments. The proposed detection setup has several advantages: it eliminates complicated instrumentation, and requires only few universal devices such as computer screen and digital camera. The total cost of the system is estimated to $\sim$400 GBP, which makes it an affordable research and testing tool. It is envisioned that – following further development and validation of the method – it may be possible to implement the proposed system in the study of other chemical and physical processes, including: diffusion, turbulence, separation, and various types of oscillating reactions.

Acknowledgements

We thank the Ministry of Science and Technology of Taiwan (formerly, National Science Council; grant no. NSC 102-2113-M-009-004-MY2), and the National Chiao Tung University for the financial support of this work. We also thank Prof. Yu-Chie Chen for lending us the fibre optic spectrophotometer.

Notes and references

1 Sigma-Aldrich, ChemFiles, 2005, 5, 7, 3–4.
2 J. Taylor and G. Veronis, *Science*, 1986, **231**, 39–41.
3 C. Almarcha, P. M. J. Trevelyan, P. Grosfils and A. De Wit, *Phys. Rev. Lett.*, 2010, **104**, 044501.
4 P.-H. Li, H. Ting, Y.-C. Chen and P. L. Urban, *RSC Adv.*, 2012, **2**, 12431–12437.
5 F. Sagués and I. R. Epstein, *Dalton Trans.*, 2003, 1201–1217.
6 I. R. Epstein, *An Introduction to Nonlinear Chemical Dynamics: Oscillations, Waves, Patterns, and Chaos*, Oxford University Press, New York, 1st edn, 1998.
7 B. P. Belousov, Сборник рефератов По радиационной медицине *(Collection of Abstracts on Radiation Medicine)*, 1959, pp. 145–147.
8 A. M. Zhabotinsky, Биофизика *(Biophysics)*, 1964, **9**, 306–311.
9 R. J. Field and M. Burger, *Oscillations and traveling waves in chemical systems*, Wiley, New York, 1st edn, 1985.
10 H. Landolt, *et al.*, *Ber. Dtsch. Chem. Ges.*, 1886, **19**, 1317–1365.
11 H. N. Alyea, *et al.*, *J. Chem. Educ.*, 1977, **54**, 167–168.
12 D. A. Skoog, F. J. Holler and S. R. Crouch, *Principles of Instrumental Analysis*, Thomson-Brooks/Cole, Belmont, 6th edn, 2006, pp. 374–379.
13 K. G. Kraiczek, R. Bonjour, Y. Salvadé and R. Zengerle, *Anal. Chem.*, 2014, **86**, 1146–1152.
14 D. A. Skoog, D. M. West, F. J. Holler and S. R. Crouch, *Fundamentals of Analytical Chemistry*, Thomson-Brooks/Cole, Belmont, 8th edn, 2003.
15 E. R. Fossum, *IEEE Trans. Electron Devices*, 1997, **44**, 1689–1698.
16 M. Kulp, P. L. Urban, M. Kaljurand, E. T. Bergström and D. M. Goodall, *Anal. Chim. Acta.*, 2006, **570**, 1–7.
17 S. Fujieda, Y. Mori, A. Nakazawa and Y. Mogami, *Adv. Space Res.*, 1999, **23**, 2057–2063.
18 C. Basavaraja, R. Pierson and D. S. Huh, *Bull. Korean Chem. Soc.*, 2009, **29**, 2241–2246.
19 R. W. G. Hunt, *The Reproduction of Colour*, Wiley, New York, 6th edn, 2004.
20 Spectral Responses, http://www.maxmax.com/spectral_response.htm.
21 Microscopy U, Spectral Imaging and Linear Unmixing, http://www.microscopyu.com/articles/confocal/spectralimaging.html, viewed on 6/5/2014.
22 E. da Nobrega Gaiao, V. Lacerda Martins, W. da Silva Lyra, L. Farias de Almeida, E. Cirino da Silva and M. C. Ugulino Aráujo, *Anal. Chim. Acta*, 2006, **570**, 283–290.
23 W. Silva Lyra, V. Bezerra dos Santos, A. G. Gama Dionízio, V. Lacerda Martins, L. Farias Almeida, E. Nóbrega Gaião, P. H. G. Dias Diniz, E. Cirino Silva and M. C. Ugulino Araújo, *Talanta*, 2009, **77**, 1584–1589.
24 E. H. Doeven, G. J. Barbante, E. Kerr, C. F. Hogan, J. A. Endler and P. S. Francis, *Anal. Chem.*, 2014, **86**, 2727–2732.
25 E. Petryayeva and W. R. Algar, *Anal. Chem.*, 2014, **86**, 3195–3202.

